J Solid State Electrochem (2005) 9: 845–849
DOI 10.1007/s10008-005-0025-7

ORIGINAL PAPER

Alexander S. Bondarenko · Genady A. Ragoisha

Variable Mott-Schottky plots acquisition by potentiodynamic electrochemical impedance spectroscopy

Received: 29 April 2005 / Revised: 9 May 2005 / Accepted: 27 May 2005 / Published online: 12 July 2005

Abstract Potentiodynamic electrochemical impedance spectroscopy provides extraction of potential-dependent space charge layer capacitance from potentiodynamic impedance spectra of non-stationary semiconductor–electrolyte interface. The new technique has been applied for acquisition of Mott-Schottky plots of cathodically treated TiO_2 anodic films. Cathodic treatment in 1 M H_2SO_4 increases donor density and flat band potential of TiO_2. Freshly doped films show hysteresis in the space charge layer capacitance in cyclic potential scans. The subsequent cycling eliminates the hysteresis but preserves the greater part of the doping effect.

Keywords Potentiodynamic electrochemical impedance spectroscopy · Multivariate electrochemical response analysis · Semiconductor-electrolyte interface · Mott-Schottky plots

Introduction

Acquisition of Mott-Schottky plots is a usual way for semiconductor materials electrochemical characterisation [1–3]. Mott-Schottky plot (inverse square of space charge layer capacitance, C_{sc}^{-2}, versus semiconductor electrode potential E gives doping density by slope of the straight line and flatband potential by intercept. Electrochemical determination of these parameters is simple when energy band edges are pinned at the surface and ac response of space charge layer capacitance can be separated in frequency range from other interfacial structures and processes, which is a usual case for stationary ideally polarisable semiconductor-electrolyte interface. Complications come with surface states and Faradaic processes that require frequency response analysis by impedance spectroscopy for extraction of space charge layer capacitance from the total ac response [3–8]. Common impedance spectroscopy is a stationary technique and this makes the problem, since complex semiconductor–electrolyte interfaces are often non-stationary, especially in microheterogeneous systems where the advantages of electrochemical characterisation could be exceptionally important.

New opportunities for non-stationary interface frequency response analysis emerge from potentiodynamic electrochemical impedance spectroscopy (PDEIS) [9, 10]. PDEIS decomposes ac responses of different interfacial processes and structures in electrode potential scan and this enables acquisition of C_{sc}^{-2} (E) plots in a single experiment. Analysis of potentiodynamic impedance spectra provided separation of overlapping double layer response and responses of non-stationary upd [11, 12] and simultaneous anion adsorption [9, 13].

This communication reports PDEIS application for non-stationary TiO_2 anodic film Mott-Schottky plots acquisition in system with variable donor density attributed to electrochemical proton intercalation and ejection. Cathodic treatment of passive anodic films on titanium is known to increase donor density by proton intercalation [14]. Though the proton intercalation effect on semiconductor properties was known to electrochemists, the non-stationary processes stayed on the by-way of semiconductor electrochemistry because of complexity of non-stationary systems frequency response analysis with common techniques. With potentiodynamic frequency response analysis, phenomena of this kind become easily traceable.

Presented at the 4th Baltic Conference on Electrochemistry, Greifswald, 13–16, 2005

A. S. Bondarenko · G. A. Ragoisha (✉)
Physico-Chemical Research Institute, Belarusian State University, 220050 Minsk, Belarus
E-mail: ragoishag@bsu.by
Tel.: +375-17-2264696
Fax: +375-17-2264696

Experimental

Potentiodynamic electrochemical impedance spectrometer is a computer program that acquires electrochemical system frequency response with virtual instruments. Variable interface is probed by streams of low-amplitude wavelets in the potential scan by means of a common potentiostat used as actuator [9, 10]. Built-in analyser solves inverse problem, and gives equivalent electric circuit (EEC) parameters dependences on the electrode potential [9, 15]. Thus, the variation of space charge layer capacitance with electrode potential is obtained straightforwardly from PDEIS spectrum analysis.

Experimental set-up in PDEIS spectra acquisition and analysis was the same as in [9, 10]. Variable frequency response was acquired in the form of 3D impedance data in the range from 23 to 877 Hz measured at 20 frequencies as function of the potential in the range between 0 and 0.6 V (vs. Ag | AgCl | KCl_{sat}.) The typical view of the virtual spectrometer interface in the stage of PDEIS spectra acquisition for the cathodically doped anodic TiO_2 film is presented in Scheme 1. EEC was obtained from PDEIS spectra with a built-in spectrum analyser as described in [9, 15]. The analyser derived the EEC by complex nonlinear least squares fitting to 2D data in constant potential sections of PDEIS spectra; however, the fitting procedures benefited from EEC verification on the potential scale and this was due to the 3D nature of the overall data. Due to variation of different processes contributions to the total ac response, ambiguities of fit that occur in 2D impedance spectra are resolved in PDEIS by examination of questionable circuits behaviour on the potential scale. Correct model gives EEC elements as smooth continuous functions of the potential with χ^2 below 10^{-4} and low relative errors for individual elements, while incorrect models can occasionally fit to certain constant potential sections but show unstable behaviour with variable potential [9]. Thus, additional variable in the fitting compensates for a short frequency range in impedance spectra. The attitude to the frequency range is different in PDEIS and in stationary EIS [9]. Stationary EIS uses wide frequency ranges in order to obtain complete EEC and enable Kramers-Kronig analysis, while PDEIS intentionally narrows the range to those frequencies where the desired component of ac response can be efficiently separated from responses of overlapping EEC elements. The most informative range for interfacial constituent responses separation is usually from several 10–1,000 Hz. Space charge layer capacitance is often easily separated from double layer and Faradaic responses in single frequency slightly above this range. However, in anodic TiO_2 films, relaxation processes in the space charge layer and on the interface give additional active and reactive EEC elements, as we will show below; therefore, the non-stationary frequency response analysis was required for C_{sc} response separation.

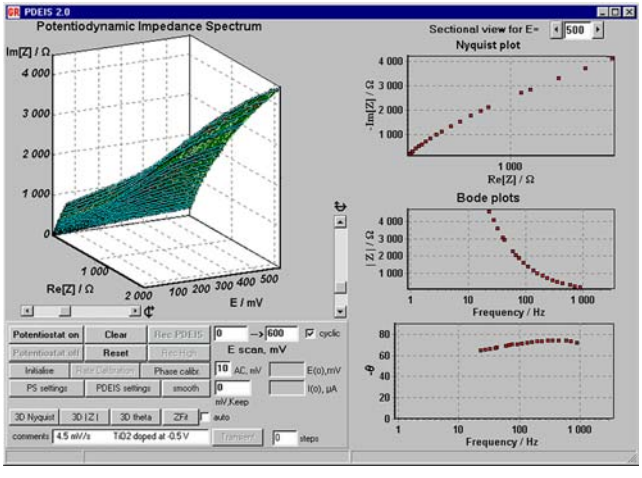

Scheme. 1 Typical view of the virtual spectrometer user interface in the stage of PDEIS spectra acquisition

We would like to note that the EECs derived from responses in short frequency ranges might differ from EECs in wide frequency range in possible lack of elements that respond outside the range tested and even in character of the derived elements, e.g. capacities that behave ideally in short frequency range are not necessarily frequency independent in wide frequency range, models of diffusion may also change with the frequency range, etc. In general, deviations from idealised models of constituent electrochemical responses increase with the frequency range; therefore the usage of narrow frequency range is wholesome for non-stationary system frequency response analysis. In PDEIS spectra analysis, the possible absence of elements that might appear in stationary impedance analysis is the advantage rather than a drawback. EEC elements that do not contribute to the response are redundant; they just increase the number of parameters and complicate inverse problem solution.

Titanium electrodes were oxidised anodically by applying a voltage up to 80 V for 10 min in 1 M H_2SO_4. The anodic film was doped by applying a cathodic treatment for 2 min at −0.5 V. After the cathodic treatment, the electrodes were kept for 20 s at 0 V and then a series of PDEIS spectra was recorded in cyclic potential scans between 0 and 0.6 V. Figures 1 and 2 show examples of constant potential sections of the PDEIS spectra and dependencies of real and imaginary impedance on electrode potential in the first cycle after doping. The analysis of PDEIS data gave the EEC shown in Fig. 3 with χ^2 of the fit around 10^{-5} and smooth continuous dependence of EEC parameters on the potential in the whole potential range. The equivalent circuit contains two capacitances (the capacitance of the space charge layer C_{sc} and the double layer capacitance C_{dl}). C_{sc} is connected in parallel with the series of an active resistance R_c and Warburg element W. C_{dl} and C_{sc} have exchanged their more common places, due to absence of Faradaic current (correspondingly, there was

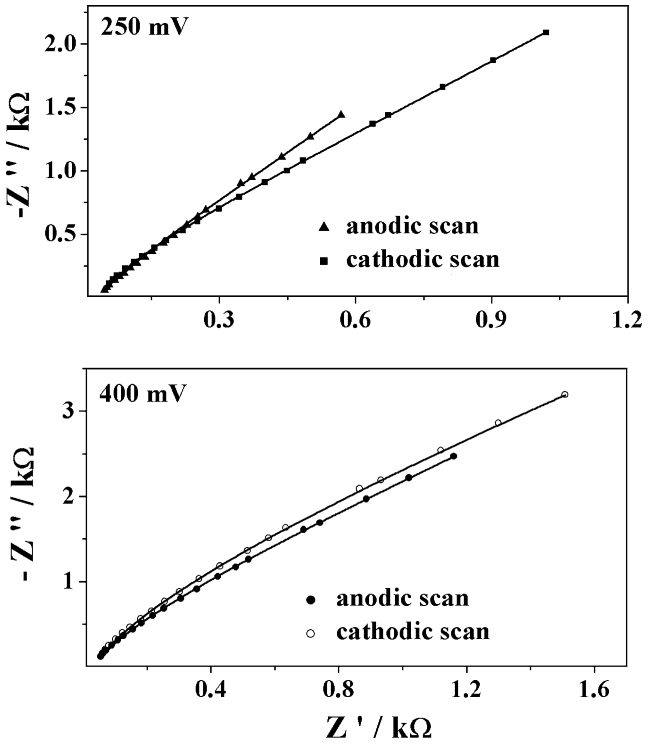

Fig. 1 Examples of constant potential sections of the cyclic PDEIS spectrum of TiO_2 anodic film in the first-cycle after cathodic doping. *Solid lines* show fit to EEC

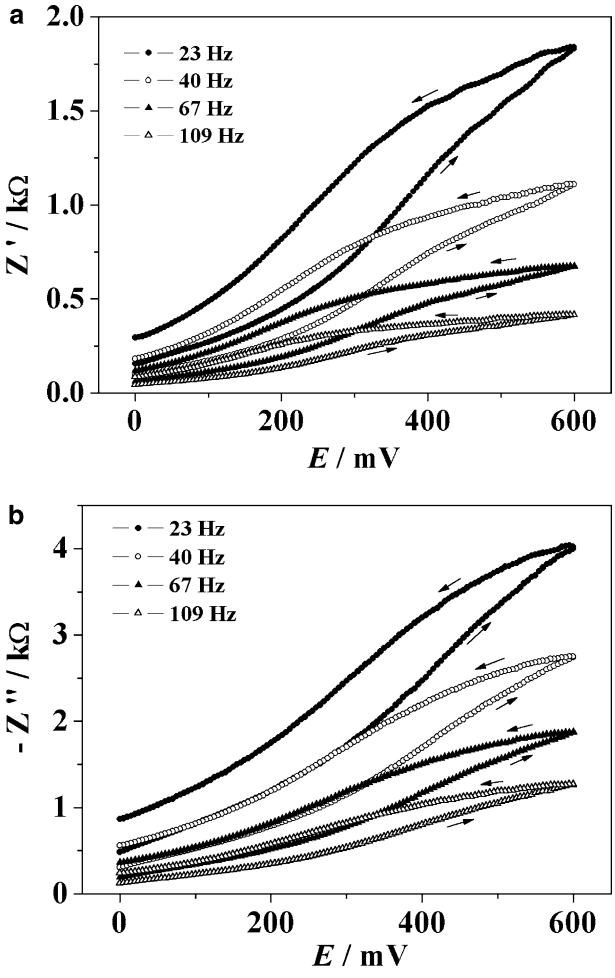

Fig. 2 **a** Real and **b** imaginary impedance variation in the first scan after cathodic doping

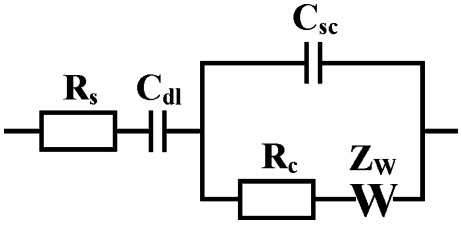

Fig. 3 The best-fit equivalent electric circuit derived from PDEIS spectrum for the variable frequency response of TiO_2 anodic film in 1 M H_2SO_4

no Faradaic impedance in parallel with C_{dl}) and non-stationary processes in the space charge layer that produced a branch similar to Faradaic impedance in parallel with C_{sc}. This additional RW contribution was almost negligible in undoped film but became considerable after the cathodic treatment. The accuracy of individual parameters determination was characterised and controlled in the EEC fit by χ^2 sensitivity to the corresponding parameter variation near the global minimum, e. g. 10% variation of χ^2 corresponded to less then 1.5% variation of C_{sc}, which was sufficient for reliable decomposition.

We acquired frequency response in the excessive mode with long-duration potential steps for precise decomposition of EEC elements. The height of each step was 5 mV and the length was 1.11 s. The ac probing signal amplitude was 10 mV, so that the resulting dependences of the parameters on the potential were quasi continuous. Using higher than usual potential steps was acceptable in this case, due to almost complete absence of Faradaic current in the potential range tested. Five millivolt steps provided relatively high overall scan rate (4.5 mV/s) with long potential steps. The main part of each period was used for frequency response probing with streams of wavelets and real-time analysis of the response, while a very small part of the period was given for updating data on a computer screen (data acquisition, processing, control and real-time visualisation of the variable response were implemented by a single processor—the CPU of a personal computer). The response in each of 20 frequencies was analysed with an individual wavelet that lasted for at least four periods of the corresponding frequency oscillation.

Results and discussion

Undoped anodic TiO_2 film gives almost identical C_{sc}^{-2} (E) plots in cathodic and anodic scans (curve 1 in

Fig. 4a). The plot is linear in the potential range from 0.15 to 0.5 V (Fig. 4b). Freshly doped TiO_2 shows non-stationarity both in constant frequencies and in constant potential sections of the PDEIS spectrum in cyclic potential scan (Figs. 1, 2). Real and imaginary impedance show a tendency towards increase and this results in the corresponding difference of C_{sc}^{-2} (E) plots in the cathodic and anodic scans (curve 2 in Fig. 4a). C_{sc}^{-2} (E) plots are non-linear for freshly doped films. In successive scans C_{sc} decreases slightly, and the difference between cathodic and anodic branches disappears. With the extinction of the rapidly damped part of the response the C_{sc}^{-2} (E) plots become linear in the potential range from 0.15 to 0.6 V (curve 3 in Fig. 4a, b).

Doping density and flatband potential are defined by Mott-Schottky relationship in the linear part of C_{sc}^{-2} (E) plot:

$$(C_{sc})^{-2} = 2(E - E_{fb} - kT/e)/N_D \varepsilon \varepsilon_0 e A^2 \quad (1)$$

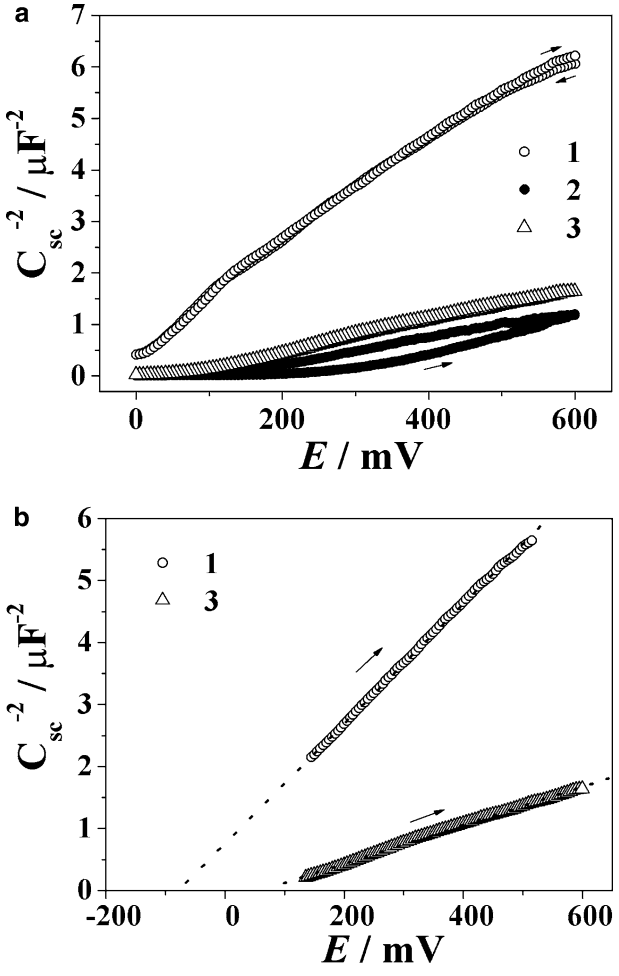

Fig. 4 **a** C_{sc}^{-2} (E) plots for anodic TiO_2 film in 1 M H_2SO_4 in cyclic potential scans; *1* before doping; *2* first scan, *3* seventh scan after 2 min cathodic treatment at −0.5 V; **b** the linear parts of the corresponding plots. $dE/dt = 4.5$ mV/s; the geometrical electrode surface area $A = 0.1$ cm^2

Where N_D is the doping density, E_{fb} flatband potential, k, the Boltzmann constant, T, the temperature, ϵ, the relative dielectric constant of the anodic film, ϵ_0, the permittivity of free space, e, the charge of an electron and A, the electrode surface.

The decrease in the slope in the cathodic treatment corresponds to increase in donor density and the positive intercept shift indicates increase in flatband potential. The doping is obviously a result of proton intercalation in the cathodic treatment, while the flatband potential variation is probably due to the concomitant change in chemical status of TiO_2 surface. E_{fb} of TiO_2 is known to depend strongly on the surface chemical status, in particular on pH-dependent hydroxyl concentration. Titanium support probably also contributed to a relatively high E_{fb} and, correspondingly, low position of band edges in terms of electron energy, both in doped and undoped films. We have examined the effect of Ti on TiO_2 thin film in the following photochemical experiment. Fifty nanometers TiO_2 film was deposited by hydrolytic decomposition of poly-butyl titanate on glass and titanium supports and 8×10^{10} mol cm^{-2} Ag^+ was adsorbed from aqueous $AgNO_3$ as described in [16]. Materials thus obtained were UV-illuminated through a mask in order to form latent image from silver clusters by photochemical reduction of Ag^+ on exposed sites and the photochemical effect was immediately amplified by selective chemical deposition of silver using a technique described in [16, 17]. Chemical amplification revealed Ag^+ photoreduction only in the film on glass support. The result of this experiment may be explained as follows. Ag^+ reduction to silver clusters requires photoelectrons with energy much above the energy level in Ag^+/Ag(bulk) system and this condition was met for photoelectrons in TiO_2 film on glass support but was not met for the film on titanium support, because of lower position of conduction energy band in the latter system.

Reversible doping of TiO_2 film by proton intercalation is characteristic for short cathodic treatment [14]. The decaying part of C_{sc} increase observed in our experiments was obviously related to surplus intercalation in very thin surface layer, thinner than the surface depletion layer. The semiconductor with strongly inhomogeneously doped surface layer does not comply with the conditions of Mott-Schottky relationship are, therefore, in freshly doped films, we did not observe linear dependence of C_{sc}^{-2} on E. In the subsequent anodic treatment, the surface excess of protons decreases and the system begins to comply with Mott-Schottky conditions.

Figure 5 shows the variations of other EEC parameters in the cathodically doped anodic film in cyclic potential scans: double layer capacitance and inverses of active resistance R_c and Warburg constant A—the variable parameter of diffusion impedance Z_W

$$Z_W = A/(j\omega)^{0.5}$$

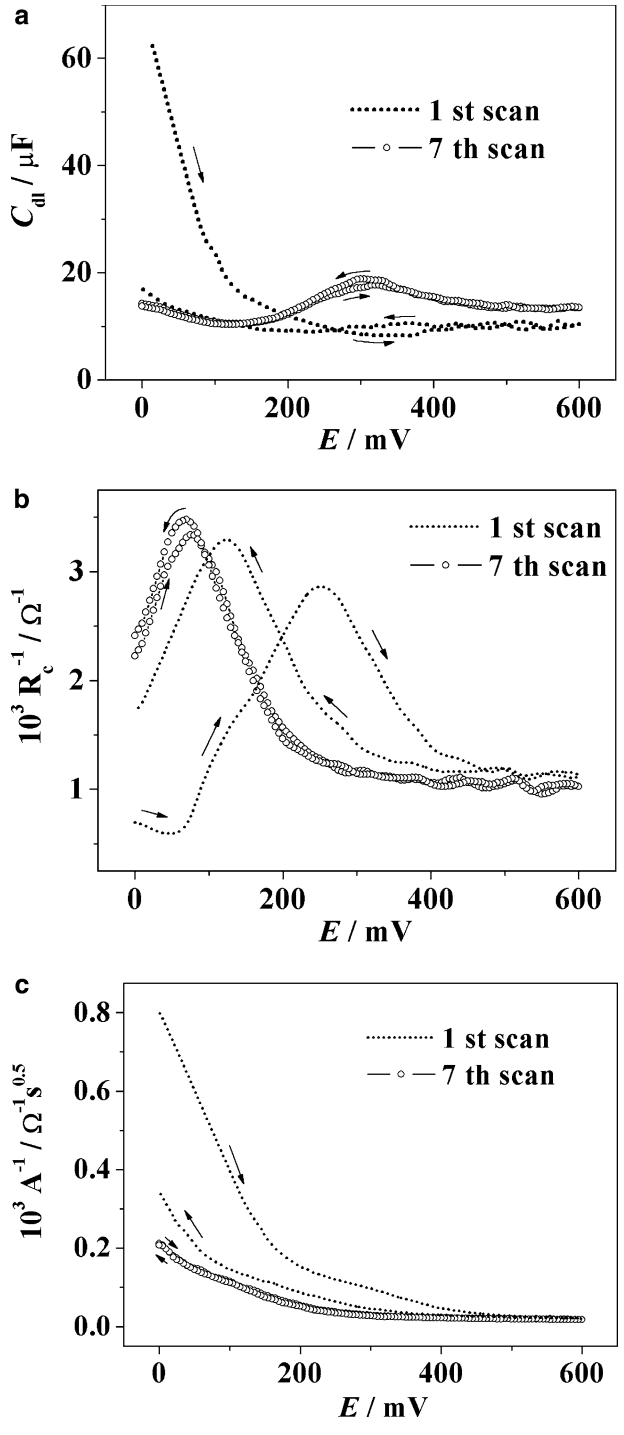

Fig. 5 Variations of **a** double layer capacitance C_{dl}, and inverses of **b** R_c and **c** Warburg constant A in cyclic scans in cathodically treated anodic film

Similarly to the space charge layer capacitance, R_c^{-1}, A^{-1} and C_{dl} show strong irreversibility in the first scan after cathodic doping and the cyclic variations of the parameters become almost reversible by the seventh scan. The residual cyclic variations of R_c^{-1} and A^{-1} originate obviously in the intercalated protons contribution to the ac response but the detailed nature of the dependences is not yet clear. Potentiodynamic impedance spectroscopy takes yet the first steps in the exploration of non-stationary semiconductor–electrolyte interfaces. In this communication, we have restricted the discussion to the intercalation effect on the space charge layer capacitance. The variations of other concurrently monitored parameters can be of interest for further research.

Conclusions

Potentiodynamic electrochemical impedance spectroscopy spectra contain information on frequency response required for decomposition of space charge layer capacitance from the overall ac response of semiconductor–electrolyte interface and also information on the effect of electrode potential. Simultaneous availability of the information on the both dependences enables fast acquisition of Mott-Schottky plots for complex interfaces. The new opportunities provided by PDEIS were used for monitoring of proton intercalation effect on semiconductor properties of anodic TiO_2 films and the analysis has revealed increase in donor density and flatband potential. The doping effect comprises a small constituent that vanishes in subsequent cycling and a larger part that remains after cycling.

Acknowledgements This work was supported by Belarusian Foundation for Basic Research (Grant H04MS-014).

References

1. Myamlin VA, Pleskov YV (1967) Electrochemistry of semiconductors. Plenum Press, New York
2. Morrison SR (1980) Electrochemistry at semiconductor and oxidized metal electrodes. Plenum Press, New York
3. Nozik AJ, Memming R (1996) J Phys Chem 100:13061
4. Blackwood DJ (2000) Electrochim Acta 46:563
5. Marsh J and Gorse D (1998) Electrochim Acta 43:659
6. Simons W, Pauwels L, Hubin A (2002) Electrochim Acta 47:2169
7. Meier A, Selmarten DC, Siemoneit K, Smith BB, Nozik AJ (1999) J Phys Chem B 103:2122
8. Gomes W, Vanmaekelbergh D (1996) Electrochim Acta 41: 967
9. Ragoisha GA, Bondarenko AS (2005) Electrochim Acta 50:1553
10. Ragoisha GA, Bondarenko AS (2003) Solid State Phenomena 90–91:103
11. Ragoisha GA, Bondarenko AS (2004) Surf Sci 566–568:315
12. Ragoisha GA, Bondarenko AS, Osipovich NP, Streltsov EA (2004) J Electroanal Chem 565/2:227
13. Ragoisha GA, Bondarenko AS (2003) Electrochem Commun 5:392
14. Schultze JW, Schweinsberg M (1998) Electrochim Acta 43:2761
15. Bondarenko AS, Ragoisha GA (2005) In: Pomerantsev AL (ed.) Progress in chemometrics research. Nova Science Publishers, New York, pp 89–102
16. Ragoisha GA (1998) Vacuum 50:69
17. Sviridov VV (1984) In: Nonsilver Photographic processes, Khimiya, Leningrad, p 242 (in Russian)